Charge Density, Covalence, and the Ground State of the $[Fe(CN)_6]^{3-}$ Ion in $Cs_2K[Fe(CN)_6]$†

Brian N. Figgis,* Edward S. Kucharski, Jacqui M. Raynes, and Philip A. Reynolds
School of Chemistry, University of Western Australia, Nedlands, W.A. 6009, Australia

Charge-density *X*-ray diffraction experiments have been performed on $Cs_2K[Fe(CN)_6]$ at 295 and 85 K. The $Fe(CN)_6$ fragment is almost octahedral in geometry, but the Cs–K environment is quite non-cubic. The Fe–CN bonding can be described by an initial $t_{2g}^5e_g^0$ Fe configuration which loses 1.4(2) e by π backbonding from t_{2g} orbitals onto the cyanide ligand and gains 1.0(2) e by σ bonding from cyanide into e_g orbitals. The observed Fe $3d$–t_{2g} distribution is anisotropic and changes little between 85 and 295 K, indicating that the cubic T_{2g} ground term of the ferricyanide ion is split by more than 200 cm^{-1}. The ground state corresponds to a spin-hole wavefunction with large $|d_{xz}\rangle$, smaller $|d_{yz}\rangle$, and negligible $|d_{xy}\rangle$ components. An analysis of e.s.r. data supports this interpretation. Polarized neutron diffraction results support the π-backbonding, σ-bonding model and emphasize the importance of both covalence and spin polarization. The ground state at 4.2 K may differ from that at 85 K, being a roughly equal mixture of $|d_{xz}\rangle$ and $|d_{xy}\rangle$, but more data are required to be certain.

The first-row transition-series hexacyanometalate-(II) and -(III) ions, $[M(CN)_6]^{4-,3-}$, form a classic series, and amongst them the ferricyanide ion, $[Fe(CN)_6]^{3-}$, is one of the best known. We have in hand a programme to study the metal–cyanide bonding in the metal(III) series because they are highly covalent in nature relative to other transition-metal complexes, and the members are sufficiently simple that we may hope to make comparisons with theoretical chemistry at a useful level. We commenced this study with the determination of the charge-[1,2] and spin-[3,4] density distributions in the $[Cr(CN)_6]^{3-}$ ion in two different compounds. We have continued with an examination of the magnetization density in the $[Fe(CN)_6]^{3-}$ ion[5] in $Cs_2K[Fe(CN)_6]$. This paper presents the complementary study, the charge density in the same crystal.

The earlier charge-density work on the $[Cr(CN)_6]^{3-}$ ion involved $Cs_2K[Cr(CN)_6]$.[1] The presence of the large Cs^+ ions stabilized the crystal in the monoclinic elpasolite structure. For the well formed crystals, such a good correction for absorption could be made that the presence of the Cs atoms was not a major limitation. The analysis showed both bonding σ and π backbonding charge transfers between chromium and cyanide, and polarization changes within that ligand probably arising from the influence of the crystal surroundings.

The *spin*-density distribution in the $[Cr(CN)_6]^{3-}$ ion from the polarized neutron diffraction (p.n.d.) experiment shows the effects of electron–electron correlation. The octahedral-symmetry ground term of the anion, $^4A_{2g}$, is essentially devoid of a contribution from orbital angular momentum. The e.s.r. g value of 1.99, isotropic and close to the spin-only value, supports that deduction.[6] No significant deviation from octahedral symmetry was detected in the anion.[3] π Backbonding of the unpaired spin and strong spin polarization in the σ framework was detected. This indicated that, to be useful, any wavefunction for the ion must take account not only of covalence but also of electron–electron correlation.

The octahedral-symmetry ground term of the $[Fe(CN)_6]^{3-}$ ion is $^2T_{2g}$, and it is well known that the contribution of the orbital angular momentum to the magnetic behaviour is substantial. The effect of small deviations from octahedral symmetry and of spin–orbit coupling combine to split the $^2T_{2g}$ term into three Kramer's doublet levels, each corresponding to different and quite anisotropic spin distributions and other properties.[7] For example the g values of $Cs_2K[Fe(CN)_6]$ are anisotropic and depart from the spin-only value substantially ($g_a = 2.55, g_b = 2.13, g_c = 1.90$).[8]

The orbital effects on the magnetic behaviour apply equally to the p.n.d. experiment, so it is possible to extract directly only the *magnetization* density. To proceed to the spin density requires a detailed knowledge of the wavefunction for the $[Fe(CN)_6]^{3-}$ ion and assumptions about the processing of the p.n.d. data.[5]

Simple analysis of the magnetization density in usual terms showed, first, considerable anisotropy in the $3d$-orbital populations of the iron atom and, secondly, strong covalence mixed with strong spin polarization, so that the spin populations on the cyanide group were complex.[5] The observed anisotropy bears some relationship to the environment of the neighbouring Cs^+ ion, and the anisotropy in populations and the strong deviation of the magnetization direction from that of the applied magnetic field resembles ligand-field model predictions.[9] The observed covalence is incompatible with the ionic ligand-field model basis, but nevertheless an improved route to the description of the spin density may be available by the use of corrections derived from the model, and is being further developed.

At the temperature of the p.n.d. experiment, 4.2 K, only the ground level is occupied and the magnetization density arises from that. At the same low temperature the neutron diffraction structure of $Cs_2K[Fe(CN)_6]$ shows that the $Fe(CN)_6$ octahedron is almost regular.[5,8] At the temperature of 85 K at which the *X*-ray data for a charge-density study were collected, the ground state of the complex ion may no longer be so simple. Several energy levels may be occupied according to a Boltzmann distribution, depending on the splitting of the $^2T_{2g}$ term. Such an alteration should be reflected in changes in $3d$-orbital populations and possibly in the molecular geometry of the $Fe(CN)_6$ unit. Further effects due to changes in the ground state, large thermal motion, or incipient phase change may occur at higher temperatures.

† Dicaesium potassium hexacyanoferrate(III).

Supplementary data available: see Instructions for Authors, *J. Chem. Soc., Dalton Trans.*, 1990, Issue 1, pp. xix—xxii.

Table 1. Crystal and experimental data * for $Cs_2K[Fe(CN)_6]$

	85(2) K	295(2) K
Crystal dimensions/mm		
Centre to (100), (−100)	0.118	0.124
(011), (0 −1 −1)	0.180	0.177
(01−1), (0−11)	0.147	0.152
(−111)	0.172	0.158
(−1−1−1)	0.158	0.157
Unit cell		
a/pm	1 104.1(4)	1 114.5(4)
b/pm	814.6(4)	813.1(4)
c/pm	759.6(2)	766.4(2)
β/°	90.49	90.16(3)
U/nm^3	0.683(1)	0.695(1)
D_m/kg l^{-1}		2.50(2)
D_c/kg l^{-1}	2.51	2.47
No. reflections measured	41 919	24 563
No. unique reflections	7 223	5 766

* Details common to both determinations: space group $P2_1/n$; $Z = 2$; λ(Mo-K_α) 71.069 pm; M 516.4; F(000) 499; $[(\sin\theta)/\lambda]_{max.}$ 10.9 nm^{-1}; μ(Mo-K_α) 6.73 mm^{-1}; transmission factors 0.16—0.30.

Experimental

In charge-density studies the properties of the crystal used for the experiment are all important. The presence of disorder, highly anisotropic thermal motion, an incipient phase change, strong extinction, or an irregular shape seriously degrade the quality of the X-ray data which can be obtained, and hence the analysis of the minor components upon which the definition of the valence features depends. It is also desirable that absorption of the X-rays be low. It is well known[10–13] that the binary alkali-metal salts of the $[M(CN)_6]^{3-}$ ions show quite strong effects of disorder, polytypism, and relatively low-temperature phase changes. Consequently, they are unsuitable for our purposes. Much the same remarks apply for crystals for use in spin-density studies using the p.n.d. technique, although the absorption problem is of much smaller importance there.

The salt we have chosen to study is $Cs_2K[Fe(CN)_6]$. Although the presence of the relatively highly X-ray absorbing and scattering Cs atoms in the structure is obviously undesirable, the other advantages of using this salt much outweigh that.

The salt $Cs_2K[Fe(CN)_6]$ was prepared by the addition of CsCl in 2:1 mole ratio to an aqueous solution of $K_3[Fe(CN)_6]$. The precipitate was dissolved in warm water and well formed rectangular prismatic red-brown crystals were obtained by slow cooling. After preliminary photographic examination, a crystal of regular shape with the dimensions set out in Table 1 was mounted on a Syntex $P2_1$ four-circle diffractometer equipped with a locally developed nitrogen gas cooling attachment. The cell constants were determined by least-squares refinement of the setting angles of six reflections of high angle chosen so as to maximize the precision. A complete sphere of data, apart from some small segments obscured by the cooling device, was collected at 85(2) K to $2\theta = 100°$. The specifications of standards, scan widths, and other diffractometer parameters have been described previously.[14] No significant change in the standards occurred during the course of the data collection. Crystal and other experimental data are given in Table 1. A further sphere of data was collected with the same specifications, except that the temperature was ambient, 295 K.

The data were processed using the XTAL system of computer programs[15] to give a Freidel-pair averaged set. Since this crystal is highly absorbing a careful correction for absorption is necessary. This was carried out by the empirical method described previously[1] in which the crystal dimensions were refined to maximize the agreement between medium-intensity equivalent reflections. The agreement obtained on merging all the data using observed e.s.d.s as weights was, at 85 K, $R_I = 0.030$, $\Sigma\sigma(I)/\Sigma I = 0.033$ for 7 223 unique reflections, and, at 295 K, $R_I = 0.027$, $\Sigma\sigma(I)/\Sigma I = 0.014$ for 5 766 unique reflections.

Models and Refinements

To obtain valence features of the charge density in molecules from X-ray data it is necessary to have an accurate account of the scattering by the core electrons. This is probably best accomplished, as here, by employing the X-ray data (X–X technique) using the high-angle data to define the core centres ('atomic positions'). The use of neutron diffraction data, while conceptually attractive, presents difficulties from the experimental point of view because, for example, of different behaviours in relation to thermal diffuse scattering. However, there are often difficulties associated with the X–X procedure. For example, we have on occasion found it necessary to refine the high- and the low-angle data separately, invoking distinctly different scale factors for each.[2] The refinement of the low-angle data using the atomic positions defined by the high-angle data then yielded the desired valence features.

Recently we suggested[16] that the cause of the discrepancy between the high- and the low-angle data for transition-metal complexes may arise from the differences in anharmonic thermal motions between the lighter ligand atoms and the heavier central metal and, possibly, other ions. In a study of $(NH_4)_2Cr(SO_4)_2{\cdot}6H_2O$[17] we found it possible to refine all the data with all the positional, thermal, and valence parameters, provided a quartic isotropic anharmonic thermal motion parameter was introduced for each atom. We follow that procedure here. Neutron diffraction data which defined such anharmonicity would be useful but would need to be of much greater extent than is usual for such experiments. Other possible sources of discrepancy between high- and low-angle data, such as scan truncation,[18] would be subsumed into the present empirical correction.

We previously described empirical two-parameter methods for correcting for extinction and for multiple scattering.[19] We follow the same procedure for the present data treatment. However, the extinction was small enough that the second of its parameters was not defined within the errors, so that was set to zero.

The core electrons of Cs, K, and Fe were modelled by standard ionic form factors[20] modified for anomalous dispersion.[21] For C and N, neutral atom form factors were used.[16] The valence electrons of the $Fe(CN)_6$ unit were modelled using essentially the same atomic orbital set as previously employed for $Cs_2K[Cr(CN)_6]$, derived from the theoretical atomic wavefunctions of Clementi and Roetti.[22] Of course, 3d and 4p form factors for the Fe^{III} atom were calculated to replace those of the Cr^{III}.

We define an orthogonal co-ordinate system with x along Fe–C(2), y approximately along Fe–C(1), and z approximately along Fe–C(3). We performed a conventional multipole refinement of the data following the procedure described in some detail for $Cs_2K[Cr(CN)_6]$,[1] but using appropriate radial functions on Fe. We call the refinement of the 85-K data R1.

In the case of $Cs_2K[Cr(CN)_6]$ and some other Cs-containing salts[19,23,24] we invoked thin 'shells' of electron density at 150 pm from the nucleus of the heavy atoms in order to explain some features of the scattering. We only use them here for the Cs atom. A simple description of the electron density in the outer parts of that atom could not be found. It obviously weakly overlaps with the neighbouring N atoms in the crystal and is

Table 2. Multipole coefficients resulting from refinement R1

Cs	(00)	0.2(2)	(10)	−1.1(1)	(1 + 1)	−1.3(1)	(1 − 1)	0.2(1)
	(20)	−0.2(2)	(2 + 1)	0.5(1)	(2 + 2)	−2.0(2)	(2 − 1)	−0.6(1)
	(2 − 2)	−0.7(2)	shell	0.7(1)				
K	(4s)	0.0(2)						
Fe	(00)	5.1(1)	(20)	−0.1(1)	(2 + 1)	0.2(1)	(2 − 1)	0.1(1)
	(2 + 2)	−0.3(2)	(2 − 2)	0.0(1)	(40)	−0.6(1)	(4 + 1)	0.1(1)
	(4 − 1)	−0.2(1)	(4 + 2)	−0.1(1)	(4 − 2)	−0.1(1)	(4 + 3)	0.3(1)
	(4 − 3)	−0.2(1)	(4 + 4)	−1.3(1)	(4 − 4)	−0.2(1)	(4s)	−0.3(5)
	K_{3d}	0.94(3)						
C(1)	(00)	3.9(3)	(10)	0.1(1)	(1 + 1)	1.4(5)	(1 − 1)	−0.2(1)
	(20)	−0.2(1)	(2 + 1)	0.0(1)	(2 − 1)	−0.2(1)	(2 + 2)	0.4(3)
	(2 − 2)	0.1(1)	K_{sp}	1.11(2)				
C(2)	(00)	3.5(4)	(10)	0.1(1)	(1 + 1)	1.7(5)	(1 − 1)	0.2(1)
	(20)	−0.2(1)	(2 + 1)	0.0(1)	(2 − 1)	0.0(1)	(2 + 2)	−0.1(3)
	(2 − 2)	0.2(1)	K_{sp}	1.10(2)				
C(3)	(00)	4.2(3)	(10)	0.0(1)	(1 + 1)	1.1(5)	(1 − 1)	−0.3(1)
	(20)	−0.4(1)	(2 + 1)	0.0(1)	(2 − 1)	0.1(1)	(2 + 2)	0.6(3)
	(2 − 2)	0.1(1)	K_{sp}	1.08(2)				
N(1)	(00)	4.8(2)	(10)	0.1(1)	(1 + 1)	−1.1(3)	(1 − 1)	−0.1(1)
	(20)	0.1(1)	(2 + 1)	−0.1(1)	(2 − 1)	0.2(1)	(2 + 2)	−0.1(2)
	(2 − 2)	0.1(1)	K_{sp}	1.06(2)				
N(2)	(00)	5.3(2)	(10)	0.0(1)	(1 + 1)	−0.9(3)	(1 − 1)	0.1(1)
	(20)	−0.1(1)	(2 + 1)	0.0(1)	(2 − 1)	−0.2(1)	(2 + 2)	0.2(2)
	(2 − 2)	−0.1(1)	K_{sp}	1.09(2)				
N(3)	(00)	5.5(2)	(10)	0.0(1)	(1 + 1)	−0.3(3)	(1 − 1)	−0.3(1)
	(20)	−0.2(1)	(2 + 1)	0.1(1)	(2 − 1)	0.1(1)	(2 + 2)	−0.1(2)
	(2 − 2)	−0.2(1)	K_{sp}	1.08(2)				

Mid-bond	Fe–C(1)	0.3(1)	Fe–C(2)	0.2(1)	Fe–C(3)	0.1(1)
Gaussian	C(1)–N(1)	1.7(4)	C(2)–N(2)	1.7(4)	C(3)–N(3)	0.9(4)

Table 3. Atomic positions ($\times 10^5$) derived from refinement R2 of $Cs_2K[Fe(CN)_6]$. The first entry is for the 85-K data, the second for the 295-K data. Thermal parameters (U) are in pm^2

Atom	x	y	z	U
Cs	25 151(1)	42 575(1)	−2 455(1)	208
	25 053(1)	43 218(2)	−2 074(2)	489
K	0	50 000	50 000	146
	0	50 000	50 000	312
Fe	0	0	0	112
	0	0	0	254
C(1)	3 283(9)	12 720(13)	−20 867(16)	174
	3 114(16)	12 796(23)	−20 758(29)	354
C(2)	4 167(9)	−19 947(15)	−12 379(14)	172
	3 874(17)	−20 010(26)	−12 492(22)	363
C(3)	16 668(11)	2 350(12)	7 495(13)	177
	16 644(33)	2 150(21)	6 864(25)	280
N(1)	5 462(10)	20 243(14)	−33 480(18)	277
	5 171(20)	20 310(29)	−33 271(41)	602
N(2)	6 832(10)	−31 868(15)	−19 950(14)	263
	6 321(23)	−31 945(42)	−19 949(32)	623
N(3)	26 642(12)	4 172(13)	12 209(15)	262
	26 503(33)	3 815(28)	11 211(34)	600

polarized by them and possibly by the K atoms. Consequently, we retained the multipolar description for the Cs atom. The Cr–C and C–N bonding densities were modelled, as before, by Gaussian functions of half-width 200 pm. The radial extents of the Fe, C, and N orbital functions were allowed to vary by introducing the scaling parameters K_{nl} in connection with the scattering vector, in the usual way. We call the valence orbital population refinement of the 85-K data R2, and the 295-K data, R3. A further valence refinement including the three t_{2g} mixing functions (*e.g.* $\langle d_{xy}|d_{xz}\rangle$ produced no significant improvement, or values for mixing parameters significant at the 2σ level.

Results

Refinement R1 had the parameters $R' = 0.047$, $R[F > 3\sigma(F)] = 0.023$, $\chi^2 = 1.15$, and projection efficiency 0.973, for 185 variables. The multiple scattering parameters were $m_1 = 100(8)$ and $m_2 = 760(40)$ counts, relative to a maximum observed count for any reflection of 3×10^6. Refinement R2 gave almost exactly the same fit for 144 variables, including 54 valence parameters, and $m_1 = 87(9)$ and $m_2 = 840(40)$; R3 gave $R' = 0.074$, $R[F > 3\sigma(F)] = 0.032$, $\chi^2 = 1.34$, projection efficiency 1.000, $m_1 = 58(8)$, and $m_2 = 416(43)$.

The experimental valence parameters, including multipole coefficients, which resulted from refinement R1 are given in Table 2. The atomic positions and averaged anisotropic thermal parameters which resulted from refinement R2 are given in Table 3, together with the values obtained at 295 K from R3. The bond lengths and angles and the shorter intermolecular contacts are given in Table 4, and the valence orbital populations, averaged to cubic symmetry, and renormalized to the total formula number of electrons, at 85 K, in Table 5. For reference, the values from the neutron structure determination of 4 K are included in Table 4.

The multipole coefficients of refinement R1 provide a somewhat better fit than do the parameters of R2, as they are greater in number and less constrained, and so give a limit against which the valence-orbital population treatment may be judged. As is usual, the valence-orbital population model is not significantly worse than the multipole treatment, and it is to be preferred because of the lower number of parameters.

Deformation-density Fourier maps, defined as $\rho_{obs.} - \rho_{spherical\ atoms}$, in the three planes containing the iron atoms and pairs of cyanide groups, *viz.* Fe–C(1)–C(2), Fe–C(1)–C(3), and Fe–C(2)–C(3), are shown at both 85 and 295 K [Figure 1(*a*)—(*c*) and (*d*)—(*f*)]. The residual density maps, defined as $\rho_{obs.} - \rho_{model}$, where the model is R2, are shown for the 85-K results in Figure 2(*a*)—(*c*).

Table 4. Bond lengths (pm) and angles (°) in the $Fe(CN)_6$ unit, and Cs · · · N 'intermolecular' contacts.* The first entry corresponds to the present results at 85 K, the second to those at 295 K, and the third to the neutron structure at 4 K (ref. 3)

Fe–C(1)	193.1(1)	Fe–C(2)	193.5(1)	Fe–C(3)	193.1(1)
	193.3(2)		193.7(2)		193.5(4)
	192.7(3)		191.3(4)		192.8(2)
C(1)–N(1)	116.4(2)	C(2)–N(2)	116.8(3)	C(3)–N(3)	116.5(2)
	116.1(4)		115.9(4)		115.5(5)
	115.4(3)		116.5(5)		116.2(2)
Fe–C(1)–N(1)	178.8(1)	Fe–C(2)–N(2)	179.0(1)	Fe–C(3)–N(3)	178.2(1)
	178.8(2)		179.3(2)		178.1(2)
	178.2(3)		179.6(2)		178.2(3)
C(1)–Fe–C(2)	90.27(5)	C(1)–Fe–C(3)	90.21(5)	C(2)–Fe–C(3)	90.20(5)
	90.26(8)		90.05(8)		90.26(8)
	90.2(1)		90.1(1)		89.9(1)
Cs · · · N(1)	329.3(2)	Cs · · · N(2)	318.5(1)	Cs · · · N(3)	332.4(2)
	331.5(3)		320.9(2)		336.6(3)
	327.7(5)		319.7(4)		328.9(5)
Cs · · · N(3)	320.7(1)	K · · · N(1)	279.3(2)	K · · · N(2)	281.6(1)
	325.3(3)		279.3(3)		281.9(3)
	318.8(4)		278.3(4)		280.2(4)
K · · · N(3)	276.9(2)				
	277.6(4)				
	275.7(4)				

* See ref. 3 for a definition of the equivalent positions involved.

Table 5. Valency-orbital population parameters from refinement R2 of the 85-K data. For Cs the multipoles were retained, as in Table 2. The second entries for C and N are for the $[Cr(CN)_6]^{3-}$ ion.[1,a] Populations renormalized to cell formula total

Cs	(00)	2.3(3)	(1 − 1)	0.1(1)	(2 + 2)	−1.7(2)	Shell	−0.7(1)
	(10)	−1.1(1)	(20)	0.0(1)	(2 − 1)	−0.6(1)		
	(1 + 1)	−1.2(1)	(2 + 1)	0.5(1)	(2 − 2)	−0.6(2)		
K	4*s*	0.3(3)						
Fe	$3d - t_{2g}$	3.6(2)	$3d$–e_g	1.0(2)	4*s*	−0.3(5)	K_{3d}	0.95(3)
C	$(sp)_1$	1.7(2)	$(sp)_2$	1.2(3)	p_π	1.2(1)	K_{sp}	1.16(2)
		1.9(2)		1.1(2)		1.5(1)		0.96(2)
N	$(sp)_1$	1.0(2)	$(sp)_2$	1.4(2)	p_π	2.1(1)	K_{sp}	1.09(3)
		1.2(2)		2.1(2)		2.2(1)		0.97(3)
Gaussian	Fe–C	0.06(4)	C–N	0.8(3)[b]				

[a] The model for the populations was different in ref. 1, and the results given there have been translated into the present formalism. [b] Gaussian function at bond centre.

Discussion

Structure.—The structure of this compound at both temperatures is very similar to that reported for it at 4 K[5] and for the chromium analogue.[1] There is an $Fe(CN)_6$ octahedron, almost but not quite regular within the errors both at 85 and at 295 K. A complex arrangement of compensating Cs^+ and K^+ ions is present, derived by distortion from a regular arrangement of K^+ ions at the vertices and Cs^+ ions in the faces of an $Fe(CN)_6$ octahedron.

At 4 K the $Fe(CN)_6$ octahedron is not quite regular, as Fe–C(2) is shorter than Fe–C(1) and Fe–C(3) at the 3σ level of significance. At 85 and 295 K Fe–C(2) is longer than Fe–C(1) and Fe–C(3). The change between 4K and the higher temperatures could arise from a change in the anisotropy of the $Fe(CN)_6$ electronic state.

Deformation-density Maps.—The deformation-density maps at 85 K (Figure 1) show features in the region of the cyanide ligands reminiscent of those reported earlier for the $[Cr(CN)_6]^{3-}$ ion in $Cs_2K[Cr(CN)_6]$,[3] but rather better defined, presumably because of the lower temperature of the experiment (85 *versus* 120 K) and the resulting lower anisotropic thermal motion. At 85 K the density distribution about each C and N atom is similar between each of the two figures in which it appears [Figure 1(*a*)—(*c*)], so that cylindrical symmetry of the ion is close. The density averaged over the three crystallographically unique CN groups is shown in Figure 3, and this is very similar to the equivalent map showing Figure 6 of ref. 3 and therewith with the theoretical deformation density for a free CN^- ion.[1] Again, the maps demonstrate no obvious sign of M–C bonding. It is encouraging that the *X*-ray charge-density studies on related compounds reproduce such relatively small features so well, even in the presence of the highly absorbing and scattering Cs atoms.

Around the iron atom the features are more distinctive, and again are better defined than for $Cs_2K[Cr(CN)_6]$. The 3*d* electronic configuration of the free Fe^{III} atom has 1.0 e in each orbital. On simple crystal-field grounds that expected for the known low-spin form of the atom in the complex ion is $t_{2g}{}^5e_g{}^0$, so that a deficiency of electron density in the Fe–C bond directions is anticipated, accompanied by an accumulation in between them, in the t_{2g} orbitals, as can be seen in the maps of Figure 1. In addition, in the *d*-orbital region, which extends to some 50 pm from the Fe atom, there is distinct deviation from cubic symmetry. The net deformation away from cubic symmetry is complex. Anisotropy in the t_{2g}-electron distribution

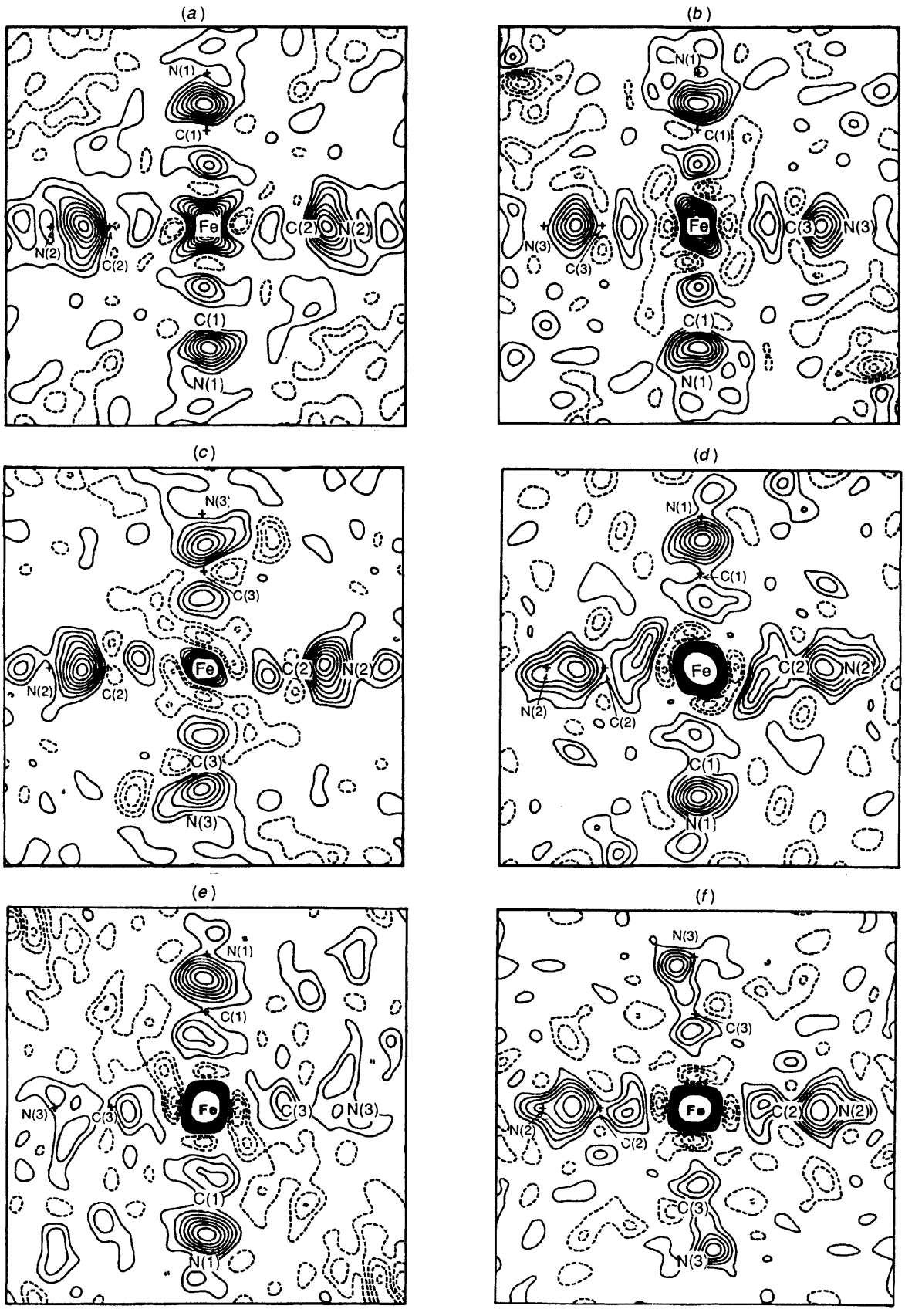

Figure 1. The deformation density in the region of the $Fe(CN)_6$ unit in $Cs_2K[Fe(CN)_6]$: (*a*) Fe–C(1)–C(2) plane at 85 K, (*b*) Fe–C(1)–C(3) plane at 85 K, (*c*) Fe–C(2)–C(3) plane at 85 K, (*d*) Fe–C(1)–C(2) plane at 295 K, (*e*) Fe–C(1)–C(3) plane at 295 K, and (*f*) Fe–C(2)–C(3) plane at 295 K. The contours are at intervals of 100 e nm^{-3}, with the zero level omitted

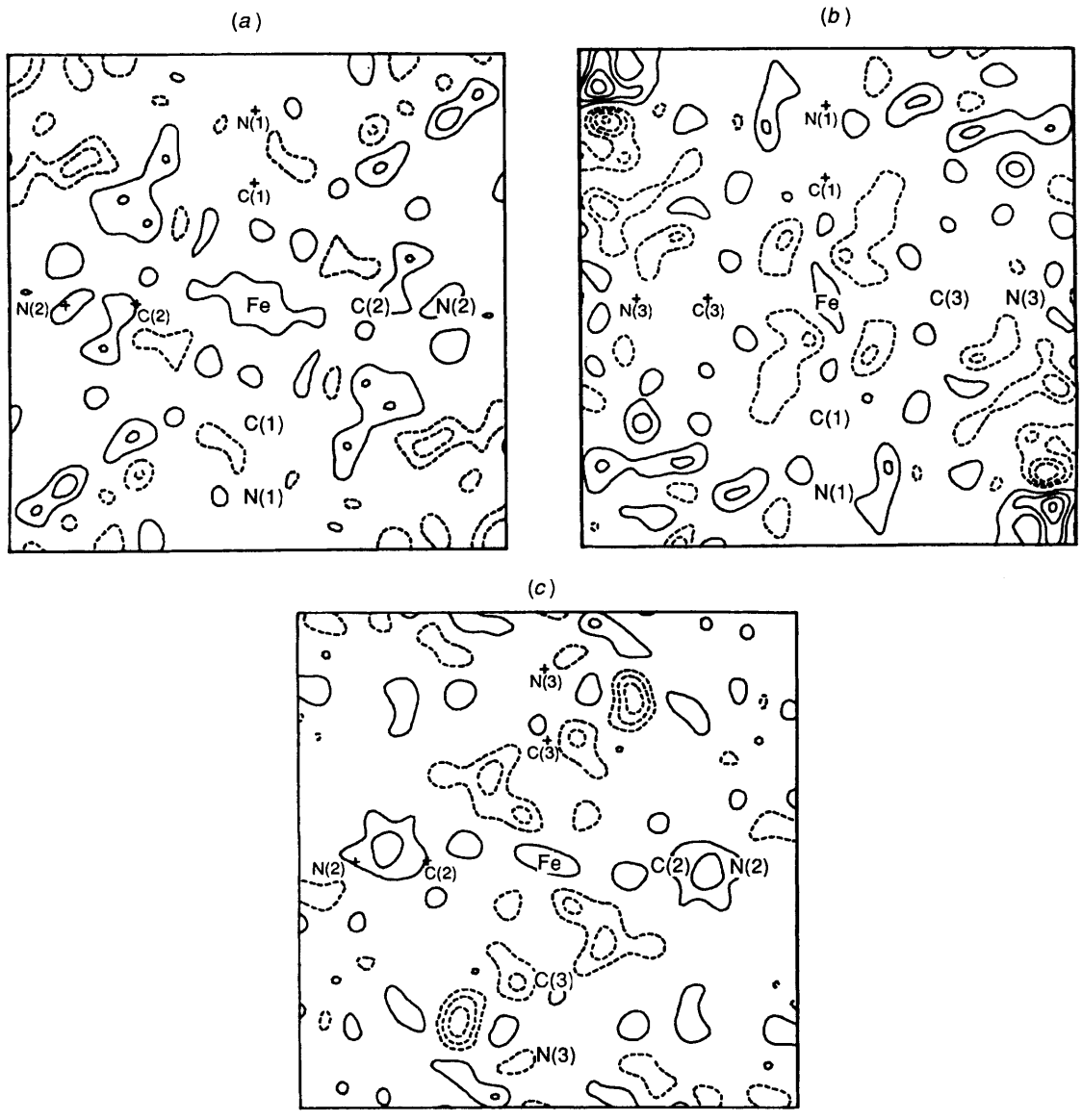

Figure 2. The residual density in the region of the $Fe(CN)_6$ unit in $Cs_2K[Fe(CN)_6]$ at 85 K: (*a*) Fe–C(1)–C(2) plane, (*b*) Fe–C(1)–C(3) plane, and (*c*) Fe–C(2)–C(3) plane. Contours as in Figure 1

may well be expected on the grounds of that demonstrated in the spin-density study[3] on the compound, which shows a marked spin anisotropy. We return to this point later.

The model residual densities shown in Figure 2 are rather flat. There is a hollow of 300 e nm^{-3} to one side of C(3)–N(3), but rather too far away to be associated directly with C–N bonding. It probably is related to the incomplete description of the Cs^+ density at a symmetry-related position. In the Fe–C(1)–C(3) plane we see residual Cs^+ density in one corner. Otherwise it seems, as would be expected from the low goodness-of-fit of R2, that the model has accounted for all the bonding features in the $Fe(CN)_6$ unit reasonably satisfactorily. However, there are t_{2g}^5-like hollows in the Fe–C(1)–C(3) and Fe–C(2)–C(3) maps at about 80 pm from the iron atom, and excess of density closer in, which avoids the Fe–C(3) direction.

The equivalent deformation-density maps from the data at 295 K [Figure 1(*d*)—(*f*)] show essentially the same features as those above, but much less distinctly because of the higher thermal motion. Deviations from cylindrical symmetry, seen for example in the C(3)–N(3) region of Figure 1(*e*), and in relative peak heights [compare C(1)–C(2) and C(3)–N(3) in Figure 1(*e*)] are noticeable. These are, however, probably the result of differences in thermal smearing between different atoms, rather than of a lowering of the symmetry of the electronic system. A similar effect has been discussed for $NiSO_4 \cdot 6H_2O$.[25]

Valence-orbital Population Refinement compared to Theory and Other Experiments.—(*i*) *The cyanide group.* As far as the cyanide ligand is concerned, at first sight the agreement between the populations derived from the earlier study on the $[Cr(CN)_6]^{3-}$ ion, and the present one, shown in Table 5, is very satisfactory. Only the $(sp)_2$ populations on N are outside the errors. However, the position is less clear because the $[Cr(CN)_6]^{3-}$ analysis included a deformation function to mimic the C–N overlap density, differing from the simple populations used in the present case. Nevertheless, the two experiments obviously describe a very similar C–N system and one which is not much different from a free CN^- ion, at least as depicted by theory (see ref. 1). We have not produced an 'at rest' difference-density map of the type shown in Figure 9 of ref. 1

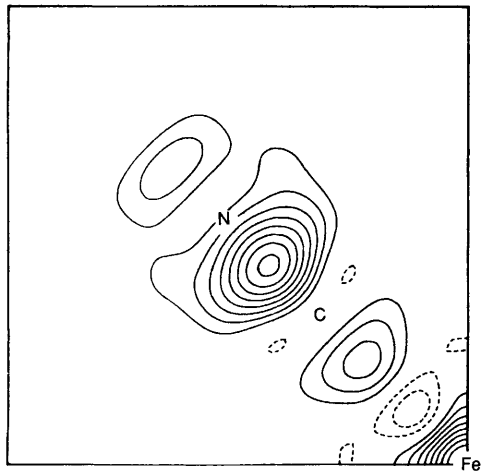

Figure 3. The deformation density in the $Fe(CN)_6$ unit in $Cs_2K[Fe^{-}(CN)_6]$, averaged over the three Fe–C–N moieties. Contours as in Figure 1

for the $[Cr(CN)_6]^{3-}$ ion. However, a cursory examination of the difference-density maps of Figure 1 or the populations of Table 5 show that the density on the N atom in the present study also shows the accumulation in the N σ-lone pair and deficiency in its π system that was notable in the chromium analogue, and was in contrast to the opposite position for the hexa-ammine and penta-ammineaqua-cobalt(III) salts of that ion. In the previous studies we attributed the majority of the changes in the cyanide ion to intermolecular polarization effects, with σ and π covalence being a smaller contributor.

(*ii*) *Covalence in the* $[Fe(CN)_6]^{3-}$ ion. In this section we restrict ourselves to discussing results averaged to octahedral symmetry. On the iron atom the valence-orbital populations show significant small differences within the t_{2g} orbitals. The effects of deviations which lower the symmetry of the $[Fe(CN)_6]^{3-}$ ion are treated in the next section, (*iii*).

There have been several previous theoretical studies of the electronic structure of the $[Fe(CN)_6]^{3-}$ ion, all of which have included restriction to octahedral symmetry. The most valuable seem to be the all-electron calculations of Sano *et al.*, one employing a standard unrestricted Hartree–Fock (UHF) treatment[26] and one the local-density approximation in the DV-Xα formalism.[27] A comparison of the predictions of those theories with the experimental results of the present work and our own DV-Xα calculations, and with the spin-density study, is given in Table 6.

On several grounds, the comparison can only be limited. First, the experiments produce least-squares fitted populations of the atomic functions used in the model, while the theories employ the conventional Mulliken population analysis of molecular-orbital composition, and the two are rather different things. Secondly, the p.n.d. experiment reflects only the ground-state wavefunction and gives a very highly anisotropic t_{2g} population, of which only the average is quoted in Table 6, while the present experiment is also anisotropic. Thirdly, of course, the experiments pertain to a real crystal, but the previous calculations to an isolated $[Fe(CN)_6]^{3-}$ ion. Fourthly, the calculations do not agree in all respects and there is the difficulty that the standard UHF does not list α and β spin populations necessary to compare with the p.n.d. experiment. Nevertheless, the comparison brings out an interesting degree of agreement, and equally interesting disagreements.

The comparison takes place between the observed and calculated charge populations *via* 'prepared atoms', *viz.* Fe $t_{2g}^{5}e_g^{0}$ and, for the cyanide ligands C $\sigma^{3}\pi^{1.5}$ and N $\sigma^{3}\pi^{2.5}$ atoms. On the iron atom the agreement with theory is not nearly as good as was seen for the $[Cr(CN)_6]^{3-}$ case. We find the t_{2g} orbitals have been strongly depleted (1.4 e), presumably by a π back donation to the cyanide group, but the theories show much less of such an effect. In better agreement is the observed movement of 1.0 e into the e_g orbitals by σ donation from the cyanide unit where the theories predict about that amount. In contrast to some other studies we have performed, here we see no diffuse (4*s*/*p*) population on the iron atom. In that regard there is consistency with the $[Cr(CN)_6]^{3-}$ result. However, the first two theories predict about 0.6 e. The 3*d* radial parameter 0.95(3) indicates a small contraction from the free-ion theoretical value. Given the large covalent charge transfers, such a change is reasonable, and the contraction is observed generally.[14] The Fe–C overlap population, 0.07 e, found is rather smaller than the theories produce, but certainly is within as good an agreement as could be expected considering the limitations mentioned above in making these comparisons.

The comparison of this experiment with the spin-density study indicates that, as we have observed elsewhere for very covalent systems, charge transfers in the bonding are much greater than the spin transfers, and the connection between the two experiments is not simple.

The observed cyanide-ion populations are quite different between the three independent units, so that only a rough comparison can be made between theory, which is for octahedral symmetry, and experiment. We note the positive spin populations of the nitrogen atoms, derived from π backbonding, and the negative populations of the carbon atoms, derived from spin polarization of the σ-bonding system, in both the theory and in the experimental results. These are just the same features we saw in the case of the $[Cr(CN)_6]^{3-}$ ion, again both in the theory and in experiment.

While our calculation reproduces experiment best of those available, nevertheless all agree in allowing a simple interpretation of the bonding. π Backbonding from Fe t_{2g} orbitals onto the cyanide ligand occurs together with a comparable amount of σ bonding from cyanide into Fe e_g orbitals. Covalence of up and down spin orbitals is different, resulting in spin polarization and no straightforward comparability of spin and charge densities.

(*iii*) *Non-cubic anisotropy around the* $[Fe(CN)_6]^{3-}$ *ion.* The spin, and less dramatically the charge, density are not of octahedral symmetry. In the somewhat related case of the $[Fe(OH_2)_6]^{2+}$ ion in ammonium iron(II) Tutton salt $[(NH_4)_2Fe(SO_4)_2{\cdot}6H_2O]$, where again there is only inversion symmetry, both experiment[28] and theory[29] require the proper treatment of the low symmetry for the best use of the available information. In this case a simple restricted Hartree–Fock wavefunction in which the hole in the Fe t_{2g}^{6} orbital set is represented as a linear combination of $|d_{xz}\rangle$, $|d_{yz}\rangle$, and $|d_{xy}\rangle$, while a great improvement on higher-symmetry models, is still not adequate to explain the p.n.d., magnetic, e.s.r., and spectroscopic information simultaneously.[28] In particular the p.n.d. experiment requires the treatment of both covalence and spin polarization for its explanation.

The 3*d* populations, both spin and charge, reflect a substantial degree of differential covalence both between up (α) and down (β) spin and between the d_{xz}, d_{yz}, and d_{xy} orbitals. Such differential covalence is shown clearly, both in the experimental comparison of spin and charge densities, and in theoretical DV-Xα calculations. It is only a rough, but nevertheless justifiable, assignment to locate the major part of the 'spin hole' by use of the lowest 3*d* charge population and highest spin population. At 85 K we observe 3*d* charge populations of 1.35(7) for d_{xy}, 1.02(7) for d_{xz}, 1.21(7) for d_{yz}, 0.56(8) for d_{z^2}, and 0.43(8) e for $d_{x^2-y^2}$. The relative order of Fe t_{2g} populations agrees well with a spin hole located mainly in $3d_{xz}$.

At 295 K, with lesser experimental accuracy, after adjusting

Table 6. Comparison of the valence-orbital population shifts (e or spin) for charge and spin experiments compared with *ab-initio* theory. The numbers quoted are relative to a 'prepared' Fe $t_{2g}^5e_g^0$ atom and C $\sigma^3\pi^{1.5}$ and N $\sigma^3\pi^{2.5}$ atoms for the cyanide ligands, and the experiments are averaged to octahedral

		Charge			Spin	
		This experiment	UHF theory[26]	DV-Xα theory[27]	Exptl.[3]	DV-Xα theory[27]
Fe	d_π–t_{2g}	−1.4(2)	−0.09	−0.38	0.86(8)	0.88
	d_σ–e_g	1.0(2)	0.96	1.7	0.10(8)	0.12
	$4s/p$	−0.3(5)	0.63	0.68	—	0.03
	K_{3d}	0.95(3)	—	—	0.911(1)	—
C		0.0(2)	−0.07	−0.45	−0.06(10)	−0.05
N		−0.4(2)	−0.14	0.12	0.02(1)	0.04
Overlap	Fe–C	0.06(4)	0.19	0.29	—	—
	C–N	0.8(3)	1.73	1.50	—	—

the e_g population to 1.0, we obtain populations of 1.33(15) for d_{xy}, 0.78(17) for d_{xz}, and 1.09(16) for d_{yz}, leading to a similar conclusion as to the state. This similarity to the 85-K result leads us to conclude that we are observing the same state at both temperatures, and that the other two components derived from the $^2T_{2g}$-split term are not significantly thermally populated. The observed σ and π charge transfers suggest that the 3*d* population of the formally occupied spin orbital is reduced to 0.66 e by π backdonation if we assume that the unoccupied orbital is increased by π donation to *ca.* 0.3 e. The 'spin hole' is thus reduced to *ca.* 0.4 e by the effects of covalence. The 295-K population while dominated by the d_{xz} hole is not sufficiently well defined experimentally to say that d_{yz} is a minor contributor.

Other experiments available relevant to the $[Fe(CN)_6]^{3-}$ ion in this temperature region are those involving Mössbauer[10] and e.s.r. spectroscopy.[8] The Mössbauer spectrum only shows that the Fe is significantly non-cubic between 80 and 295 K. However the e.s.r. *g* tensor can be interpreted in terms of a simple Fe t_{2g} spin-hole model. While, because of the neglect of spin polarization and differential covalence, this can only be an approximation, it is useful. The e.s.r. theory for a t_{2g}^5 system is well known and has been summarized in ref. 30. The principal elements of the observed e.s.r. *g* tensor in the molecular frame of the $Fe(CN)_6$ unit are $g_x = 2.19, g_y = 1.94$, and $g_z = 1.49$. There is ambiguity in the solution since only the absolute values of *g* are measured. However, one reasonable solution is a spin-hole wavefunction $\psi = 0.99\,|d_{xz}\rangle + 0.14\,|d_{yz}\rangle - 0.08\,|d_{xy}\rangle$, with an orbital reduction factor of $k = 0.9$. We thus obtain the same qualitative conclusion as from the charge-density experiment.

When we turn to the p.n.d. results a more confused picture emerges. The orbital magnetization complicates any interpretation. However we have shown that the details of the magnetization density conform qualitatively to that expected from the Cs^+ cation arrangement.[5] The 3*d* spin populations of $|d_{xy}\rangle = 0.72(5)$, $|d_{xz}\rangle = 0.78(6)$, and $|d_{yz}\rangle = -0.64(8)$ again indicate a state containing $|d_{xz}\rangle$, but also $|d_{xy}\rangle$ and $|d_{yz}\rangle$. It may be that in the 4.2-K structure the $|d_{xz}\rangle$ and $|d_{xy}\rangle$ spin states are so close in energy that spin–orbit coupling and configuration interaction produce a ground state with *ca.* 50% of each. It is, however, clear that spin polarization and orbital effects are so severe that a better treatment of orbital magnetization and further experimentation, both p.n.d. and e.s.r. spectroscopy, are necessary before we can be definite that a substantial change in ground state occurs between 80 and 4.2 K.

Acknowledgements

The authors are grateful to the Australian Research Grants Scheme for financial support.

References

1 B. N. Figgis and P. A. Reynolds, *J. Chem. Soc., Dalton Trans.*, 1987, 1747.
2 B. N. Figgis and P. A. Reynolds, *Inorg. Chem.*, 1985, **24**, 1864.
3 B. N. Figgis, J. B. Forsyth, and P. A. Reynolds, *Inorg. Chem.*, 1987, **26**, 101.
4 B. N. Figgis and E. S. Kucharski, unpublished work.
5 C. A. Daul, P. Day, B. N. Figgis, H. U. Gudel, F. Herren, A. Ludi, and P. A. Reynolds, *Proc. R. Soc. London, Ser. A*, 1988, **419**, 205.
6 T. Mitsuma, *J. Phys. Soc. Jpn.*, 1961, **16**, 1796.
7 J. Baker and B. N. Figgis, *Aust. J. Chem.*, 1982, **35**, 265.
8 P. J. Brown, P. Day, P. Fischer, H. U. Gudel, F. Herren, and A. Ludi, *J. Phys.*, 1982, **43**, C235.
9 B. N. Figgis and C. D. Delfs, unpublished work.
10 S. R. Fletcher and T. C. Gibb, *J. Chem. Soc., Dalton Trans.*, 1977, 309.
11 B. N. Figgis, B. W. Skelton, and A. H. White, *Aust. J. Chem.*, 1978, **31**, 1195.
12 R. R. Ryan, J. R. Smith, and B. I. Swanson, *Acta Crystallogr., Sect. B*, 1979, **35**, 264.
13 B. N. Figgis, P. A. Reynolds, and G. A. Williams, *Acta Crystallogr., Sect. B*, 1981, **37**, 504.
14 B. N. Figgis, P. A. Reynolds, and S. Wright, *J. Am. Chem. Soc.*, 1983, **105**, 434.
15 J. M. Stewart and S. R. Hall (Editors), 'The XTAL System of Crystallographic Programs,' Computer Science Technical Report TR-901, University of Maryland, College Park, Maryland, 1986.
16 P. A. Reynolds and B. N. Figgis, *Aust. J. Chem.*, 1989, **42**, 1831.
17 B. N. Figgis, E. S. Kucharski, and P. A. Reynolds, *Acta Crystallogr.*, 1990, in the press.
18 R. Destro, *J. Appl. Crystallogr.*, 1980, **13**, 425.
19 B. N. Figgis, E. S. Kucharski, and P. A. Reynolds, *Acta Crystallogr., Sect. B*, 1989, **45**, 232.
20 'International Tables for Crystallography,' eds. J. A. Ibers and W. C. Hamilton, Kynoch Press, Birmingham, 1974, vol. 4.
21 D. T. Cromer and D. J. Lieberman, *J. Chem. Phys.*, 1970, **53**, 1981.
22 E. Clementi and C. Roetti, *At. Data Nucl. Data Tables*, 1974, **14**, 187.
23 B. N. Figgis, P. A. Reynolds, and A. H. White, *J. Chem. Soc., Dalton Trans.*, 1987, 1737.
24 C. D. Delfs, B. N. Figgis, E. S. Kucharski, and P. A. Reynolds, *J. Chem. Soc., Dalton Trans.*, 1989, 1779.
25 G. J. McIntyre, H. Plasiewicz-Bak, and I. Olovsson, *Acta Crystallogr., Sect. B*, 1990, **46**, 51.
26 M. Sano, H. Kashiwagi, and H. Yamatera, *Inorg. Chem.*, 1983, **21**, 3873.
27 M. Sano, H. Adachi, and H. Yamatera, *Bull. Chem. Soc. Jpn.*, 1981, **54**, 2898.
28 B. N. Figgis, J. B. Forsyth, E. S. Kucharski, P. A. Reynolds, and F. Tasset, *Proc. R. Soc. London, Ser. A*, 1990, **428**, 113.
29 R. Doerfler, *J. Phys. C*, 1987, **20**, 2533.
30 R. E. De Simone, *J. Am. Chem. Soc.*, 1973, **95**, 6238.

Received 8th March 1990; *Paper* 0/01055C